JOURNAL OF GEOPHYSICAL RESEARCH, VOL. 97, NO. E10, PAGES 15,967–15,976, OCTOBER 25, 1992

Pancakelike Domes on Venus

DAN MCKENZIE

Institute of Theoretical Geophysics, Department of Earth Sciences, Cambridge, England

PETER G. FORD, FANG LIU AND GORDON H. PETTENGILL

Center for Space Research, Massachusetts Institute of Technology, Cambridge

The shape of seven large domes on the plains of Venus, with volumes between 100 and 1000 km^3, is compared with that of an axisymmetric gravity current spreading over a rigid horizontal surface. Both the altimetric profiles and the horizontal projection of the line of intersection of domes on the synthetic aperture radar images agree well with the theoretical similarity solution for a Newtonian fluid but not with the shape calculated for a rigid-plastic rheology nor with that for a static model with a strong skin. As a viscous current spreads, it generates an isotropic strain rate tensor whose magnitude is independent of radius. Such a flow can account for the randomly oriented cracks that are uniformly distributed on the surface of the domes. The stress induced by the flow in the plains material below is obtained and is probably large enough to produce the short radial cracks in the surface of the plains beyond the domes. The viscosity of the domes can be estimated from their thermal time constants if spreading is possible only when the fluid is hot and lies between 10^{14} and 10^{17} Pa s. Laboratory experiments show that such viscosities correspond to temperatures of 610° to 700°C in dry rhyolitic magmas. These temperatures agree with laboratory measurements of the solidus temperature of wet rhyolite. These results show that the development of the domes can be understood using simple fluid dynamical ideas and that the magmas involved can be produced by wet melting at depths below 10 km, followed by eruption and degassing.

1. INTRODUCTION

The plains of Venus contain large numbers of small domes [*Head et al.*, 1991; *Pavri et al.*, this issue] that were probably formed by the extrusion of viscous magmas from central conduits. Similar structures are found on Earth where rhyolitic and dacitic magmas are extruded [see *Fink*, 1987], and those on Venus are also likely to be formed from silicic magmas containing more than 60% SiO_2. We chose seven large domes for detailed study. The largest is in Rusalka Planitia, and it is close to the equator where the altimeter footprint along the track is only 2 km. Since the diameter of this dome is 34 km, its shape can be accurately measured with the altimeter on Magellan. The other six domes illustrated in Figure 1 are at about −30°N and are all smaller than that in Rusalka Planitia. One altimeter track crosses close to the axis of one of these domes but does not provide a detailed profile because the footprint spacing is about 5 km.

Several suggestions have been made to account for the observed shapes of silicic domes on Earth. *Huppert* [1982] argued that they were produced by an axisymmetric gravity current spreading over a rigid horizontal surface and calculated the profile of such a dome when the rheology is that of a viscous fluid. If, however, the rheology of the magma is better described by that of a Bingham fluid with a yield stress [see *Fink*, 1987; *Blake*, 1990], then the shape of the dome is described by the expression obtained by *Nye* [1952]. Another model for such domes was proposed by *Iverson* [1987] and by *Fink and Griffiths* [1990]. They argued that the magma viscosity obtained by using *Huppert's* [1982] expressions is unrealistically large and that the dome shape is instead controlled by stresses within a thin skin of cool, highly viscous material that forms at the surface of the dome. Since the altimeter on Magellan can measure the cross section of the dome in Rusalka Planitia to an accuracy of about 100 m, a profile across this dome can be used to test these three models and in this way to constrain the mechanisms that control the shapes of domes on Venus and the rheology of magmas involved.

We first show that the profile of the dome in Rusalka Planitia agrees well with that expected from *Huppert's* [1982] model but not with that calculated from a rigid-plastic rheology. A static model with constant surface tension also does not give a shape that agrees with the observed profile. We then show that a viscous model can also account for the observed shape of the curve of contact between two overlapping domes, and for a number of other features on the synthetic aperture radar (SAR) images. *Huppert's* [1982] expressions allow the viscosities of the magma involved to be estimated, and the values obtained are similar to those measured in the laboratory. This agreement in turn allows the temperature of the magma to be estimated if its composition is that of a rhyolite (rhyolite and granite are extrusive and intrusive rocks of the same composition). The temperatures obtained in this way agree with that found in the laboratory for the wet solidus of such a magma. Finally, we speculate about the geological processes within Venus that may generate the silicic magmas that form the domes.

2. DOME PROFILES

In plan view the seven domes are almost perfectly circular and have radii that are large compared with their heights (Figure 2). Their shape suggests that they were formed by eruption from central conduits whose maximum width

Paper number 92JE01349.
0148-0227/92/92JE-01349$05.00

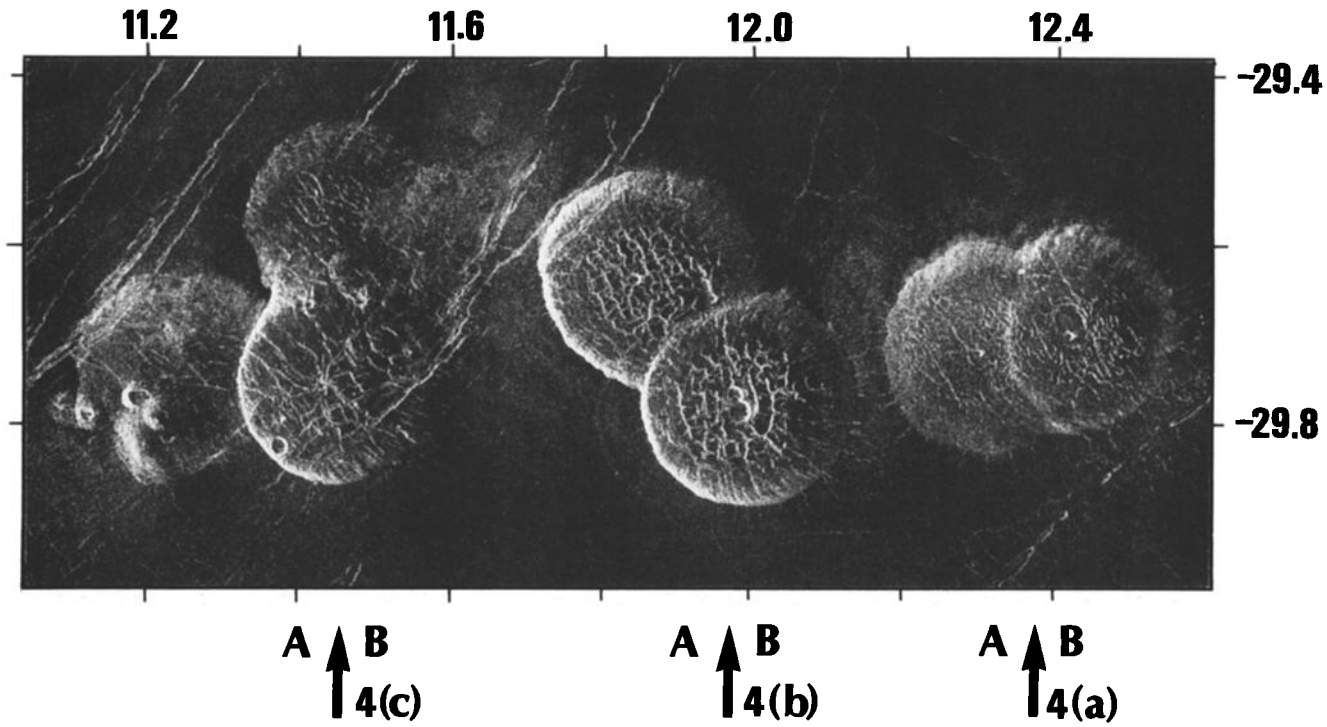

Fig. 1. A SAR image of the domes east of Alpha. The pairs of domes that are shown in plan view in Figure 4 are marked by labelled arrows.

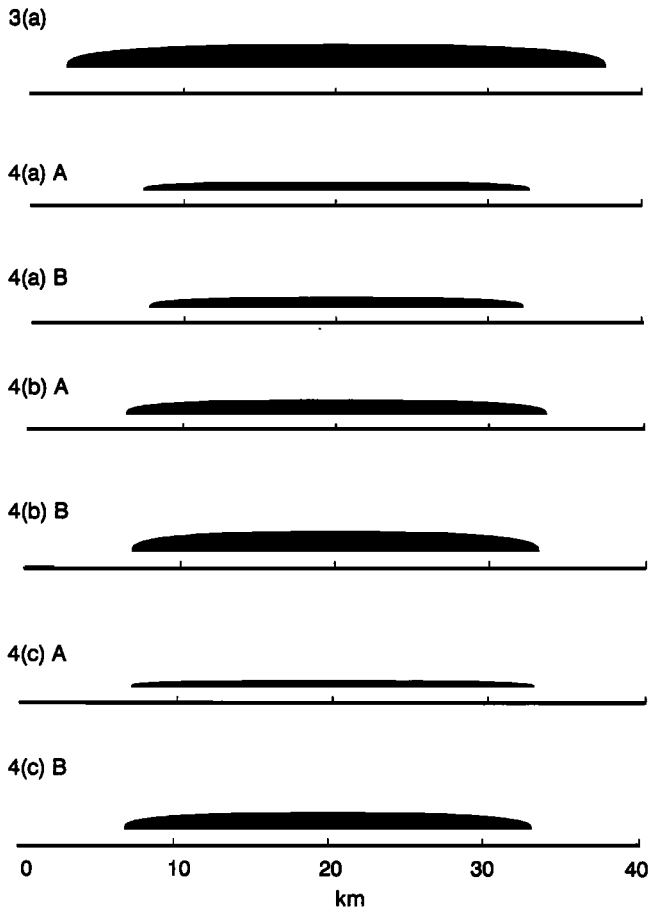

Fig. 2. Sections without vertical exaggeration through the centers of the domes in Table 1.

was small compared with the present radii of the domes. Their circularity requires the surface onto which they were erupted to have been planar and horizontal. We examine three models that have been proposed to account for the shape of similar domes on Earth. In two of these the rate of release of gravitation energy by the spreading of the dome is restricted by internal stresses. These are viscous stresses in *Huppert's* [1982] model and stresses causing plastic failure in *Nye's* [1952] rigid-plastic model. In the third model that we consider, the spreading tendency is resisted by constant tension in a thin surface skin.

The spreading of an axisymmetric viscous drop of fluid over a rigid horizontal surface has been studied in some detail by *Huppert* [1982], who shows that the height h of the surface of a dome is related to the radial distance r from its center by

$$h = h_0 \left(1 - \left(\frac{r}{r_0}\right)^2\right)^{1/3} \quad (1)$$

where h_0 is the height at $r = 0$ and r_0 is the radius of the dome. This expression is only valid when $r_0 \gg h_0$ and does not apply near the edge of the dome where $r_0 - r < h_0$. Equation (1) applies only when the volume of magma in the dome is constant and will therefore not describe dome growth. However, Huppert found experimentally that the shape described by equation (1) was rapidly established when fluid ceased to be supplied to the dome and also argued on theoretical grounds that any initial shape would asymptotically approach this similarity solution. Equation (1) should therefore provide a good approximation to the shape when the duration of the eruption τ_e is short compared with the thermal time constant τ_c of the dome. We will for simplicity assume that $\tau_c \gg \tau_e$, but there is at present no evidence that this assumption is correct for Venusian domes.

Figures 3*a*-3*e* show two profiles that were chosen because they pass close to the center of a large dome in Rusalka Planitia (Figure 3*e*). Such a restriction is important, both because Doppler sharpening of the radar pulse returned to the altimeter can only reduce the size of the footprint in the direction that is along the track and because the shape of the center of the dome is most strongly affected by its rheology. The size of the footprint in the across-track direction cannot be improved by Doppler sharpening and is never better than 15-30 km. Profiles must therefore cross close to the center of the dome, where the approximation that the shape changes only slowly in the cross-track direction is likely to be satisfied, if the shape of a dome is to be accurately measured at intervals that are small compared to 15 km. The dome in Figures 3*a*-3*e* is close to the equator of Venus (Table 1), where the spacecraft is close to the planet and therefore its horizontal velocity is large. For both these reasons the spacing between the Doppler sharpened footprints of the altimeter is only about 2 km and shows how effectively this technique can increase the spatial resolution of the altimeter [*Ford and Pettengill*, this issue]. *Huppert's* [1982] model was also used to fit the profile across the dome east of Alpha shown in Figure 3*f* at a latitude of about −30°N. At this latitude the footprint spacing increases to about 5 km because Magellan is farther from the planet and is travelling more slowly. This profile therefore provides a less severe test of any theory of dome formation than do those across the dome in Rusalka Planitia.

Two values of r_0 were first estimated by measuring the location of the dome center on the digital SAR image and of the two points where each altimeter track crossed the margin of the dome. The values of r_0 and h_0 were then found by fitting equation (1) to the altimeter profiles by least squares, with the requirement that r_0 lay between the two estimates obtained from the SAR image. Once r_0 and h_0 are known the volume Q of a dome is easily obtained by integration of equation (1)

$$Q = \frac{3\pi}{4} h_0 r_0^2 \tag{2}$$

and is listed in Table 1. The rms misfits are 51 m for orbit 3067, and 90 m for 1277. It is not straightforward to compare these misfits with estimates of the likely errors in the heights measured by the altimeter, because these are strongly dependent on the reflection properties of the Venusian surface. If the reflection is from a smooth horizontal surface, the error is governed by the pattern of phase modulation of the radar and is no more than a few meters. However, if the surface is rough, the shape of the returned pulse is controlled by energy scattered from regions that are not directly beneath the track of the spacecraft. Doppler sharpening can remove returns from regions ahead or behind the spacecraft, but the returned pulse is still broadened by scattering from regions at right angles to the spacecraft velocity vector. This effect controls the accuracy with which the arrival time of the reflected pulse can be measured. The surface of the domes is rough and strongly affects the shape of the returned pulse. Therefore the likely error in height along the profiles in Figure 3 is probably as great as 100 m, and the differences between the observed and the calculated shapes in Figure 3*a* and 3*c* are unlikely to be significant.

An alternative model for the rheology of a silicic magma is that of a rigid-plastic material, and the shape of a dome with such a rheology was obtained by *Nye* [1952]. Using the same notation as before, his expression is

$$h = h_0 \left(1 - \frac{r}{r_0}\right)^{1/2} \tag{3}$$

and has a discontinuity in dh/dr at $r = 0$. Since the shear stress in the plastic region is independent of strain rate, the dome shape calculated for such a rheology is independent of the eruption rate. *Blake* [1990] has carried out a number of experiments with a suspension of clay in water that has a rheology similar to that of a rigid-plastic material and found that Nye's expression provides a good fit to his experiments (notice that Blake uses the same symbol R to denote both r and $r_0 - r$). However, as Figures 3*b* and 3*d* show, Nye's expression does not fit the altimeter observations. The rms misfit is 121 m for the profile from orbit 3067 and 165 m from orbit 1277. Therefore the ability of a profile to discriminate between the two rheological models is greater when the track passes close to the center of a dome (Figure 3*e*).

The third model that has been proposed to account for the shape of silicic domes depends on the strength of a thin skin of cool material at the surface of the dome [*Iverson*, 1987; *Fink and Griffiths*, 1990]. These authors argued that the magma viscosity calculated from *Huppert's* [1982] expressions [see *Huppert et al.*, 1982] was much greater than that observed in the laboratory, and therefore that some process other than viscous spreading must be involved. However, *Webb and Dingwell* [1990] have recently measured viscosities of 10^{14} Pa s in dry rhyolite melts at a temperature of about 700°C, and therefore this objection to Huppert et al.'s proposals no longer applies (see below). It is nonetheless of interest to discover whether a thin strong skin under constant tension can account for the observed shapes. To do so, we used the differential equations given by *Iverson* [1987] that are satisfied by any radial profile and retain his notation

$$\frac{d\eta}{dr'} = z' - \frac{\eta}{r'} \tag{4}$$

$$\frac{dz'}{dr'} = \frac{\eta}{\sqrt{1-\eta^2}} \tag{5}$$

where

$$r' = \frac{r}{\sqrt{\sigma t/\rho g}}, \quad z' = \frac{z}{\sqrt{\sigma t/\rho g}}, \quad \eta = \sin\phi$$

σ is the shear stress within the skin of thickness t, ρ is the melt density, g is the acceleration due to gravity, r is the radial and z is the vertical coordinate, and ϕ is the angle between the tangent to the surface and the horizontal. Following Iverson, z was taken to increase downwards, which is the opposite convention to that used by Huppert. Equations (4) and (5) were used when $|\phi| \leq \pi/4$. When this condition was not satisfied,

$$\frac{dr'}{dz'} = \frac{\mu}{\sqrt{1-\mu^2}} \tag{6}$$

$$\frac{d\mu}{dz'} = -z' + \frac{\sqrt{1-\mu^2}}{r'} \tag{7}$$

were used instead, where

$$\mu = \cos\phi$$

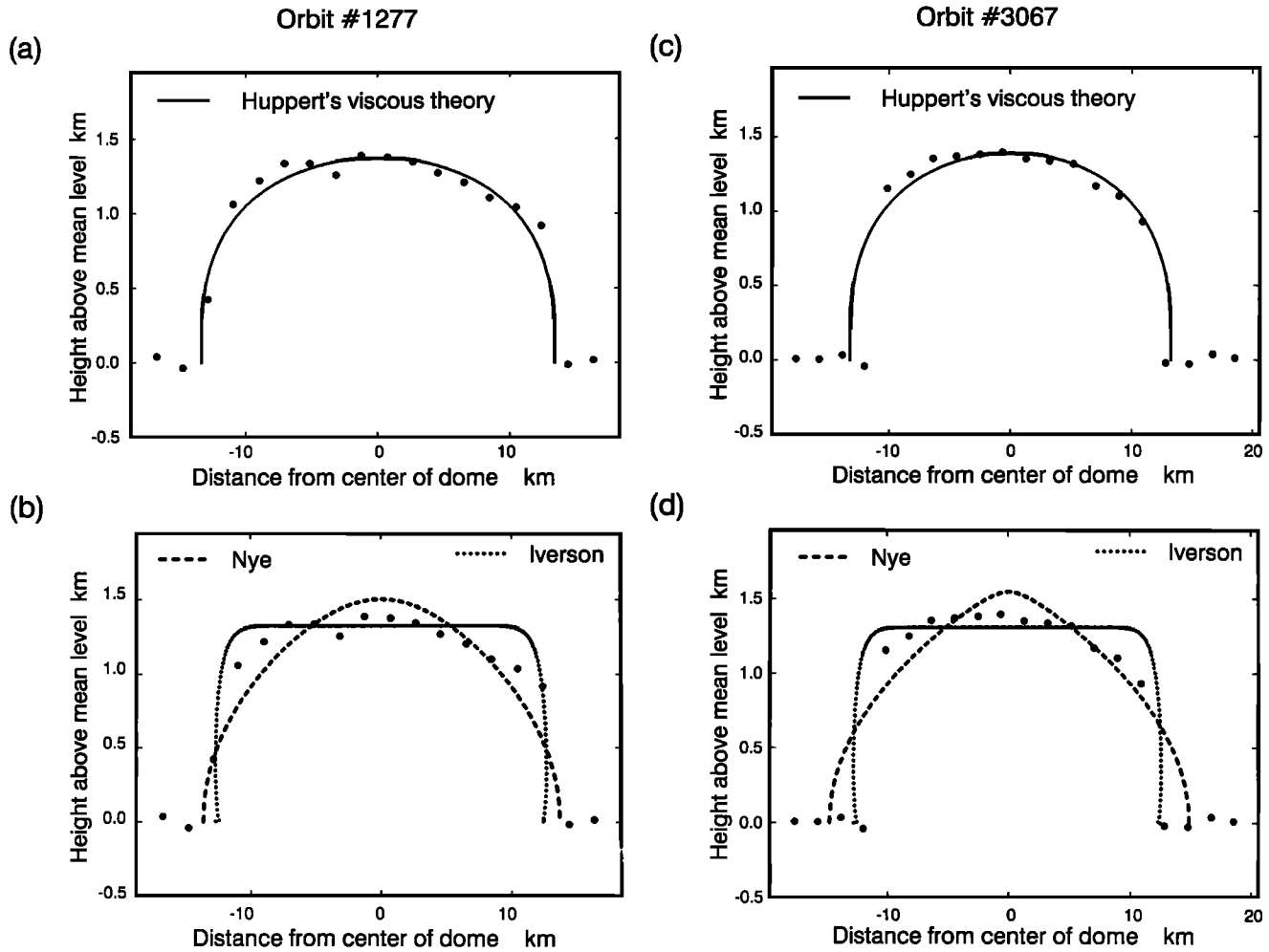

Fig. 3. (*a*) Altimeter profile across the dome in Rusalka Planitia from orbit 1277, shown in Figure 3*c*, from footprint 627 on the left to 644 on the right, plotted as a function of the distance along the track, with the origin at the point of closest approach to the center of the dome (Table 1). The heavy line shows the best fit obtained using equation (1) for a newtonian viscous rheology and the parameters in Table 1. (*b*) The same profile as Figure 3*a*, with the best fitting curve for a rigid-plastic rheology from equation (3), shown by the heavy dashed line. The dotted line shows a skin model with a similar aspect ratio to that observed, obtained by integrating equations (4)-(7) with $h' = 3 \times 10^{-8}$. (*c*) and (*d*) As for Figures 3*a* and 3*b*, but for orbit 3067, from footprint 670 on the left to 688 on the right. Two points at the level of the plains plot inside the calculated profile of the dome because the echo from the plains was so much stronger than that from the edge of the dome that the time of arrival of the latter could not be measured. (*e*) Ground track of the altimetric profiles in Figures 3*a*-3*d*. The continuous circle shows the radius of the dome obtained from fitting orbit 1277, the dashed circle that from 3067. (*f*) A profile from orbit 576 from footprint 1454 on the left to 1461 on the right, across the western of the two most easterly domes east of Alpha (see Figure 4*a* for the altimeter track). The heavy line shows the best fitting model with Newtonian viscosity.

Integration was started with $\eta = 0$ and $z' = h'$, where

$$h' = \frac{h}{\sqrt{\sigma t/\rho g}} \tag{8}$$

and h is the height of the origin of the coordinate system above the center of the dome, and first used equations (4) and (5), changing to (6) and (7) when $\phi > \pi/4$, then back to (4) and (5) when $|\phi| \leq \pi/4$. Integration was stopped when $|\phi| < 0.01$. A scheme similar to that of Iverson's was used, except that all four equations were integrated using a fourth-order Runge-Kutta integration, and 0.5 was replaced by 1.0 in two places in line 1920 of his code.

The value of h' in equation (8) is the dimensionless height above the center of the dome at which the pressure within the fluid of the dome would be zero. Integration of the equations starting with various values for h' showed that the aspect ratio, defined to be the ratio of the radius to the height of the dome, was ~ 1 unless h' was very small. The observed aspect ratio of the dome in Figures 3*b* and 3*d* is about 10 and could only be reproduced with a value of h' of between 10^{-8} and 10^{-9}. The top of the dome is then very flat. Such a result is to be expected from the behavior of drops of mercury, whose shape is controlled by a constant surface tension, and therefore satisfies equations (4)–(7). When such drops are small, they are approximately spherical, but the top of large aspect ratio pool of mercury is sufficiently flat to act as mirror that reflects with little distortion.

Figures 3*b* and 3*d* show that the profile of a dome whose shape is maintained by a constant skin tension does not agree well with that observed. It is of course possible to maintain a dome of any shape by suitable forces within a

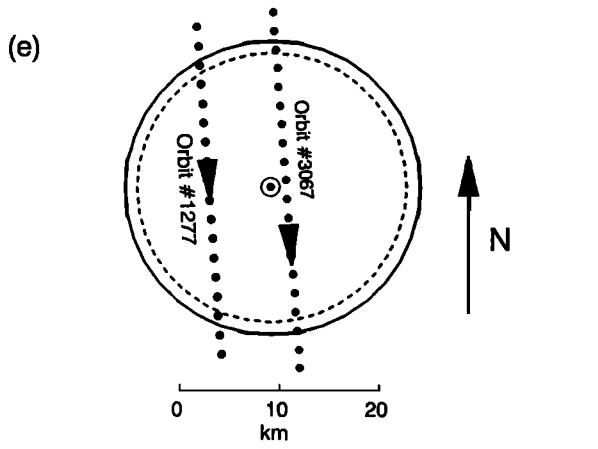

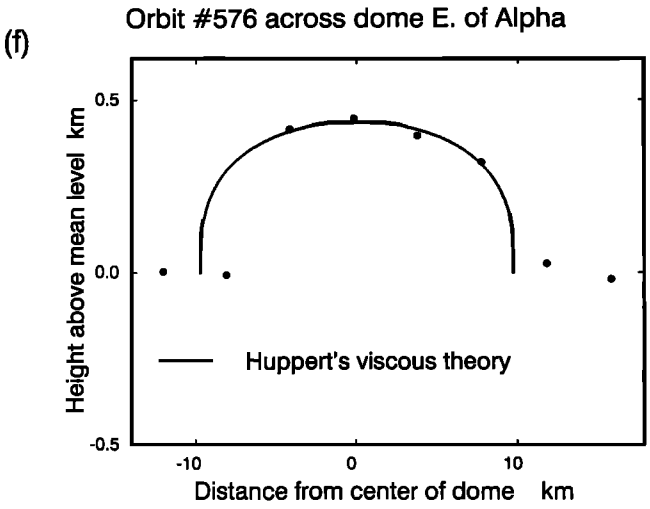

Fig. 3. (continued)

thin skin. However, the shape is only uniquely defined by the value of h' if the tensional force within the skin is required to be constant. *Iverson* [1987] imposed this condition but did not explain the physical process by which this state is maintained. His model assumes that it is the strength of the skin, rather than the fluid mechanics of melt transport, that controls the shape of the dome. However, it is unclear how such a dome could grow, since its volume could only change if the skin were to break. Once it did so, the magma would rapidly flow through the break and produce the type of composite flow seen in *Fink and Griffiths'* [1990] photographs. No such structures are visible on the domes on Venus.

Figure 3*f* shows the best fit to one of the domes illustrated in Figure 4*a*, with a rms misfit of 11 m. Though the fit is good, the 5-km spacing between the altimetric footprints is too large to provide a good test of *Huppert's* [1982] model. An attempt was also made to use a profile from orbit 571, across a large dome in Tinatin Planitia at 12.10°N, 7.63°E. Unfortunately, both the dome and the surrounding plains have been deformed and tilted since it was emplaced. It is not obvious how such effects can be removed, and unless they are, fitting the calculated profile to that observed is meaningless.

These three comparisons between the calculated and observed shapes of the Venusian domes show that the viscous model of *Huppert* [1982] best fits the altimetric profiles. The other two models are therefore not further discussed. Though the dynamics of the spreading appear to be controlled by viscous forces, rather than by the properties of the cold skin, such a skin must be present.

3. Dome Intersections and Surface Features

The altimeter profiles discussed in the last section provide the most direct test of the various models that have been proposed to account for the shape of the magma domes. However, the SAR images can also be used for this purpose, because the position of the line that marks the junction between two overlapping domes depends on their shapes. Equation (1) allows the projection of this line onto a horizontal plane to be calculated analytically from the radii r_1 and r_2 of the two domes, their central heights h_1 and h_2, and x_1 the separation of their centers. If the origin of the coordinate system is taken to be at at the center of dome 1, and the $+x$ direction to be along the line joining the centers of the two domes, then the horizontal projection of the line of intersection between the two domes forms an arc of a circle whose center is at

$$(-x_1/\beta r_2^2,\ 0) \tag{9}$$

with radius R given by

$$R^2 = \frac{\alpha^3}{\beta}\left(\frac{1}{\beta}\left(\frac{x_1}{r_1 r_2}\right)^2 + 1\right) - \frac{1}{\beta} \tag{10}$$

where

$$\alpha = h_1/h_2, \quad \beta = \frac{\alpha^3}{r_1^2} - \frac{1}{r_2^2}$$

The intersection is a straight line when $\beta = 0$, or $r_1^2/r_2^2 = h_1^3/h_2^3$. The values of h_1 and h_2 were obtained from the altimetric observations, and r_1, r_2 and x_1 were calculated from the positions of three points on the edge of each dome. Mercator projections of three pairs of domes in Figure 4 show

TABLE 1. Domes

	Figure	Latitude, deg	Longitude, deg	Radius, km	Height, km	Volume, km^3	η, Pa s	T,† °C	τ_c, years
Rusalka 1277	3*a*	-2.867	150.890	17.2	1.48	1040	1.0×10^{17}	610	7400
Rusalka 3067	3*c*	-2.867	150.890	15.8	1.40	820	8.9×10^{16}	610	6600
Alpha E	3*f*	-29.726	12.305	13.4	0.44	186	3.7×10^{14}	700	650
Alpha E	4*a*, A	-29.726	12.305	12.7	0.55	209	1.3×10^{15}	670	970
Alpha E	4*a*, B	-29.711	12.428	12.3	0.67	237	3.6×10^{15}	660	1400
Alpha C	4*b*, A	-29.632	11.854	13.7	0.97	428	1.9×10^{16}	630	3000
Alpha C	4*b*, B	-29.781	11.999	13.3	1.26	514	7.8×10^{16}	610	5100
Alpha W	4*c*, A	-29.747	11.432	12.9	0.45	176	4.5×10^{14}	690	650
Alpha W	4*c*, B	-29.736	11.223	13.1	1.05	457	3.1×10^{16}	620	3500

†The temperature estimated from equation (24).

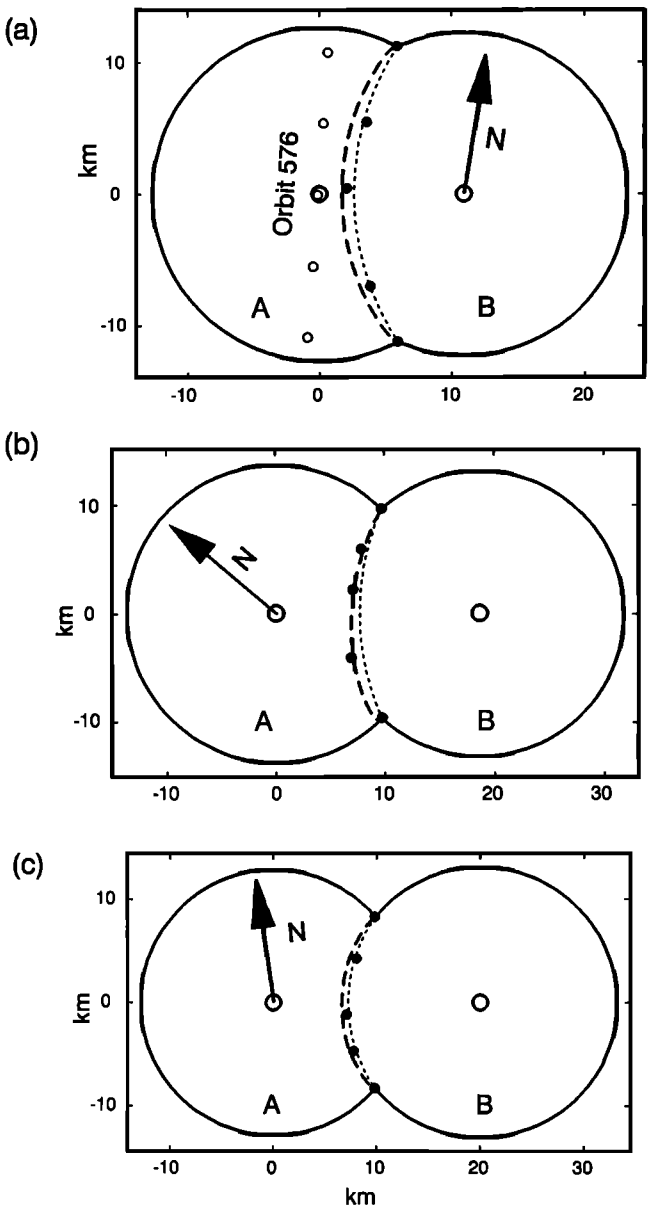

Fig. 4. (*a*) The heavy lines show the Mercator projection of the outline of the eastern pair of domes in Figure 1. The centers, shown by the larger open dots, are 10.91 km apart, and the x axis has an azimuth of 80.46°. The fine dashed line shows the projection onto the horizontal plane of the line of intersection of the two domes, that with heavy dashes shows the intersection line after the slant range correction has been applied, using an azimuth of 84.74°, measured clockwise from N, and an inclination of 30.3° for the illumination, both measured at the domes. The solid dots are points on the intersection measured from the SAR images. The arrow labeled N shows the northward pointing vector. (*b*) As for Figure 4*a*, but for the two center domes in Figure 1. The dome centers are 18.66 km apart, and the x axis has an azimuth of 140.68°. (*c*) As for Figure 4*a*, but for the two western domes in Figure 1. The dome centers are 20.03 km apart, and the x axis has an azimuth of 97.26°.

the shape of the calculated intersect lines. However, they cannot be directly compared with the SAR image, because the apparent position of a feature on the surface depends on the height of the feature as well as on the viewing angle from the spacecraft. This correction depends both on the azimuth and the angle between the line joining the spacecraft to the feature and the vertical, measured on the surface of Venus. The heavy dashed lines in Figure 4 show the position of the intersection curves after this correction has been applied, and they agree well with those observed in all three cases. Such agreement is surprising, since the flow during the emplacement of the second dome in each pair must be influenced by the presence of the first. Indeed, the original aim of the calculation of the shape of the line of intersection was to discover which of the two overlapping domes was emplaced first. The agreement between the calculated and observed lines suggests that the presence of the first dome has only a minor influence on the flow that emplaces the second and that it is therefore not easy to discover which is the older dome of each pair from their shapes alone. An experimental test of these results can easily be carried out in the laboratory, and such a program has recently been started by H. E. Huppert (personal communication, 1992). Preliminary results suggest that the shape of viscous spreading domes is indeed rather little affected by obstacles in their path.

The good agreement between the calculated and observed shapes suggests that the velocity field calculated by *Huppert* [1982] can be used to study the evolution of the domes. He shows (equation 2.19) that the radial velocity u is

$$u(r,z,t) = -\frac{\rho g}{2\eta}\frac{\partial h}{\partial r}z(2h-z) \tag{11}$$

where ρ ($\simeq 2.4$ Mg m^{-3}) is the density and η the viscosity of the dome magma, and g ($= 8.87$ m s^{-2}) is the acceleration due to gravity. The radial velocity at the surface of a dome is therefore

$$u(r,h,t) = \frac{3r}{16t} \tag{12}$$

where t is the time since the emplacement of the dome, and the three components of the horizontal strain rate tensor $\dot{e}$ are

$$\dot{e}_{rr} = \frac{\partial u}{\partial r} = \frac{3}{16t}, \quad \dot{e}_{r\phi} = 0, \quad \dot{e}_{\phi\phi} = \frac{u}{r} = \frac{3}{16t} \tag{13}$$

where ϕ is now the azimuthal angle. Since the radial and azimuthal strain rates are equal and $\dot{e}_{r\phi}$ is zero, the surface of the dome undergoes uniform extension at the same rate in all directions. Furthermore, the strain rate is independent of the radius. The SAR images of the domes in Figure 1 show that some of their central regions contain a number of irregular cracks that do not have any preferred orientation. They are also uniformly distributed over the central region of the domes. The strain rate described by equation (13) can produce such cracks in the cooler crust of the dome as the interior continues to flow. Because the horizontal strain rate tensor is isotropic and independent of radius, the cracks should not show any preferred orientation, nor should their density vary with radius. The cracks form within a thin cold layer of high viscosity at the surface of the dome whose influence on the flow is ignored in *Huppert's* [1982] calculations. That such an approximation is valid is suggested by the good agreement between the predicted and observed shapes. There is also some evidence that the formation of such cracks is influenced by the viscosity and temperature of the dome-forming magma. Of the domes east of Alpha, the three thickest domes, whose viscosity is highest and temperature is lowest, are the two illustrated in Figure 4*b* and dome B in Figure 4*c*. These are the three with the most obvious cracks in Figure 1.

The SAR image also shows that radial striations are present near the margins of the domes. Though the approximations made in deriving equation (1) fail in this region, *Huppert's* [1982] expressions for the velocity show that $\dot{e}_{\phi\phi} \gg \dot{e}_{zz}$ and $\dot{e}_{z\phi} = 0$. Hence vertical cylindrical surfaces undergo almost uniaxial extension in the azimuthal direction. Such a strain rate acting on a surface inclined to the horizontal could produce radial tension fractures like those observed.

Figure 1 shows that the plains just beyond the outer edge of several of the domes are cut by small short radial extensional fractures spaced at intervals of 2-3 km around the perimeters of the domes. No associated thrusting is visible. These fractures probably result from stresses induced by the spreading of the domes over the plains. The force/unit area f_i that acts on a surface whose normal is n_j is

$$f_i = \sigma_{ij} n_j$$

The shear stresses σ_{rz} and $\sigma_{z\phi}$ are easily calculated from equation (11)

$$\sigma_{rz} = \frac{\eta}{2}\left(\frac{\partial u}{\partial z} + \frac{\partial v}{\partial r}\right)_{z=0}, \quad \sigma_{z\phi} = 0 \tag{14}$$

where v is the vertical velocity. Since

$$\frac{\partial u}{\partial z} \gg \frac{\partial v}{\partial r} \tag{15}$$

substitution gives

$$\frac{\partial u}{\partial z} = \frac{2g\rho h_0^3 r}{3\eta r_0^2 h} \tag{16}$$

and hence

$$\sigma_{rz} = \frac{g\rho h_0^3 r}{3r_0^2 h} \tag{17}$$

An estimate of the magnitude of $\partial u/\partial z$ and σ_{rz} can be obtained by substituting

$$r \sim r_0, \; h \sim h_0$$

to give

$$\frac{\partial u}{\partial z} \sim \frac{g\rho h_0^2}{\eta r_0}, \quad \sigma_{rz} \sim g\rho h_0 \frac{h_0}{r_0} \tag{18}$$

Since the normal stress σ_{zz} is $g\rho h_0$, $\sigma_{zz}/\sigma_{rz} \sim \lambda$, where $\lambda = r_0/h_0$ is the aspect ratio of the dome. Substitution of $h_0 = 0.5$ km and $r_0 = 13$ km gives $\sigma_{zz} \sim 11$ MPa and $\sigma_{rz} \sim 0.4$ MPa. The stress field imposed by the spreading domes on the plains material is independent of the viscosity, is in the radial direction, and increases monotonically with radius. Though *Huppert's* [1982] expressions give an infinite value for σ_{rz} at the edge of the dome, they are not valid when $r_0 - r < h_0$. Nonetheless, the real radial stress exerted by the dome near its margin must be large. Such a stress produces an extensional stress within the plains beneath the domes, and a radial compression beyond their margins, where the fractures are visible. Failure in extension can only occur on planes that are normal to the least principal stress, whereas failure in shear occurs on planes at approximately 45° to the greatest and least principal stresses. Beyond the dome margins the planes on which extensional failure can occur are radial and vertical, whereas those on which thrusting may take place are tangential to the dome margin, and dip at about 45°. Whether failure will occur depends on the resistance of the material over which the domes are spreading to the two modes of failure. If it is similar to that where Venera 13 and 14 landed, its yield strength is less than 25 MPa [*Surkov et al.*, 1984], and it is likely to fail in the manner observed. The fracture geometry visible on Venus just beyond the edge of the domes differs from that observed at Mount St. Helens [*Chadwick et al.*, 1988] in several ways. On Venus the fractures are short and radial with no visible thrusts. At Mount St. Helens, extensive thrusting occurred in association with the radial fractures, and *Chadwick et al.* [1988] argued that both were produced by stresses on the walls of the vertical conduit that supplied the dome with magma. A similar origin for those on Venus is unlikely: they extend only a few kilometers beyond the edge of the domes, a distance that is small compared with the dome radius. The spacing between adjacent fractures is also small compared with the dome radius. It is more likely that the spacing between the fractures is controlled by the thickness of a weak layer near the surface.

The viscosity of the magma is an important parameter that can also be estimated from the shape of the domes. *Huppert's* [1982] equation (2.23) gives

$$\left(\frac{1}{3}\rho g Q^3 t/\eta\right)^{-1/8} r_0 = \xi_N \tag{19}$$

where η is the viscosity and

$$\xi_N = \left(\frac{2^{10}}{3^4\pi^3}\right)^{1/8}$$

Equation (19) can be used to estimate η if t is known. The viscosity of the magma depends exponentially on temperature [*Webb and Dingwell*, 1990], and therefore spreading will effectively cease when the magma cools. The time scale τ_c for such cooling is

$$\tau_c \sim \frac{h_0^2}{\pi^2 \kappa} \tag{20}$$

where $\kappa (\simeq 10^{-6}\ \mathrm{m^2\ s^{-1}})$ is the thermal diffusivity. The values for h_0 in Table 1 give characteristic thermal times of 700 to 7000 years. Setting $t = \tau_c$ in equation (19) gives

$$\eta = \frac{g\rho h_0^2 Q^3}{3\pi^2\kappa}\left(\frac{\xi_N}{r_0}\right)^8 \tag{21}$$

Equation (21) was used to obtain the estimates of η in Table 1. This rather crude theory is useful as a guide to the likely order of magnitude of the viscosity.

4. Comparison with Laboratory Experiments

It is important to discover if the properties of the magma that forms the domes on Venus are consistent with laboratory determinations of magma properties. The rheological experiments that are most suitable for this purpose are those of *Webb and Dingwell* [1990], who measured the viscosity of fibers formed from silicate melts with a variety of compositions. They were particularly interested in whether a viscous rheology could describe the creep behaviour of the melt. Their measurements on rhyolite were more extensive than those on other compositions and will be used for comparison with viscosity estimates from Venus. Though there is no direct evidence that the dome-forming magma on Venus is a rhyolite, basaltic magmas crystallize at temperatures where their viscosity is very much lower than those listed in Table 1.

Webb and Dingwell [1990] found that the strain rate of rhyolitic magmas varied linearly with stress provided the strain rate $\dot{e}$ was less than $\dot{e}_c$, where

$$\dot{e}_c \sim \frac{10^{-3} K_\infty}{\eta} \tag{22}$$

where K_∞ is the steady state bulk modulus ($\simeq$ 25 GPa) and η is the viscosity as $\dot{e} \to 0$. The strain rate can be estimated from equation (18) and the values of ρ and g used previously

$$\frac{\partial u}{\partial z} \sim 3 \times 10^6/\eta \tag{23}$$

whereas equation (22) gives $\dot{e} \sim 3 \times 10^7/\eta$. Therefore, the calculated strain rate is sufficiently low for the rheology to be described by a Newtonian viscosity, except close to the margin of the domes where *Huppert's* [1982] approximations are anyway not valid. This conclusion is consistent with the argument in section 2, which also suggested that the relationship between stress and strain rate was linear.

Webb and Dingwell's [1990] results can also be used to estimate the temperature of the magma from its viscosity if it is of rhyolitic composition. The viscosities they measured ranged from about 10^9 to 10^{14} Pa s, and the temperature variation was described by

$$\log_{10} \eta = 2.298 \times 10^4/(T + 273) - 9.15 \tag{24}$$

where T is the temperature in degrees Celsius. Equation (24) was used to calculate the magma temperatures in the last column of Table 1, which range from 610° to 700°C. If the melt composition was that of an andesite, these temperatures would be about 40°C lower [*Webb and Dingwell*, 1990]. It is unexpected and important that these temperature estimates are similar to the solidus temperature of wet rhyolite. Figure 5 compares the temperature range from Table 1 with the wet granite solidus listed by *Merrill et al.* [1970] and shows that wet melting of such material between pressures of 0.2 and 2.5 GPa can produce magmas of suitable temperature to account for the Magellan observations. Such magmas will lose most of their water when they are erupted onto the surface of Venus, and their viscosity will then increase by a factor of as much as 10^8. However, the fraction of water exsolved is only about 4%, and detailed calculations show that adiabatic expansion of the exsolved gas produces a temperature change of less than 10°C in the magma. Such degassing could account for the small crater that is visible at the center of each dome in Figure 1. Though *Webb and Dingwell's* [1990] experiments show that magmas of other compositions can also satisfy the viscosity estimates, the temperatures required are lower than those for a rhyolitic melt, whereas the wet solidus temperatures of other compositions are either the same as that for granite or are higher. Only if the melt composition is that of a granite do the temperatures estimated from the viscosities agree with the solidus temperature.

Webb and Dingwell's [1990] measurements can also be used to estimate the viscosity of the dome material at the surface temperature of Venus of about 450°C. Substitution into equation (24) gives $\eta \simeq 4 \times 10^{22}$ Pa s. This estimate is uncertain, because it requires a much greater extrapolation of Webb and Dingwell's experimental results than do the temperature estimates in Table 1. The magma is also likely to crystallize as it cools, an effect that will greatly increase its viscosity. Despite these reservations, the estimate from equation (24) is probably a useful lower bound on the likely viscosity and can be used to discover how long the domes can retain their shape. Equations (1) and (11) give V, the horizontal velocity at the outer edge of the dome

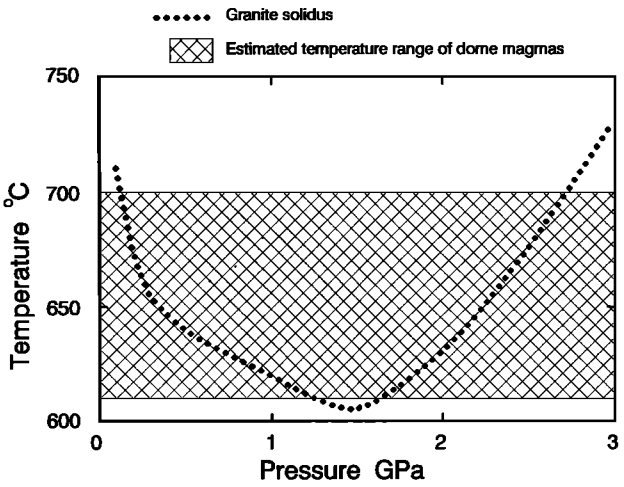

Fig. 5. The temperature range estimated from the viscosity in Table 1, compared with the solidus for wet granite from Table 2 of *Merrill et al.* [1970].

$$V = \frac{\rho g h_0^3}{3\eta r_0} \tag{25}$$

Substitution of $h_0 \simeq 1$ km, $r_0 \simeq 10$ km gives $V \simeq 1$ m/m.y. Such a velocity is sufficiently small to allow the domes to persist for times that are comparable to that of the age of the planet. Such a conclusion is also consistent with the presence of fault offsets that cross the domes. The northwestern of the two central domes east of Alpha Regio in Figure 1 is cut by a fault that crosses the plains and displaces the edge of the dome downwards and northwestwards. The fault can only produce a sharp fault scarp if the dome is no longer spreading at a significant rate. Though the velocity estimated from equation (25) is likely to be too large, it is nonetheless sufficiently small to allow fault scarps to persist for very long periods.

5. Discussion

The simple fluid dynamical model of a viscous fluid spreading over a rigid surface can account for most of the features seen on the SAR images and altimeter profiles of the pancakelike domes on Venus in some detail. These observations provide better constraints on the rheological properties of viscous magmas undergoing flow on a large scale than do any yet obtained from the Earth. The viscosity estimates in Table 1 are a weighted average of the effective viscosity that governs the evolution of the domes. In practice, the viscosity of the magma must vary strongly with depth and time. Because of the success of the simple constant viscosity model, a study of axisymmetric spreading within a cooling dome whose viscosity varies with temperature is well worth while. Such laboratory experiments have been carried out by M. V. Stasiuk (personal communication, 1992) and show that the change in the profile of the dome produced by a temperature-dependent viscosity is not large. Relative to

the constant viscosity case, temperature dependence causes the dome to become slightly flatter in the middle and steeper at the edges. Laboratory experiments of *Webb and Dingwell* [1990] allow the magma temperature to be estimated from the viscosity. If the magmas are rhyolitic in composition, the temperature estimates are similar to those of the wet solidus at depths of 10 km or more beneath the surface. Though there are no direct measurements of the composition of the dome-forming magma, the observations are all compatible with it being that of a rhyolite. The viscosity of magmas with less SiO_2 than a rhyolite have too low a viscosity at their solidus temperatures to produce the observed shapes.

The SAR and altimeter observations provide no information about the geological processes that produced the dome magmas, and the domes are not obviously related to any nearby structures. Table 1 shows that the magma volumes involved are between 10^2 and 10^3 km^3. Comparably sized explosive eruptions of silicic magma on Earth occur relatively frequently and were produced by Toba (2800 km^3 [*Rose and Chesner*, 1987]), Yellowstone (eruptions of 2500 km^3, 1000 km^3, and 280 km^3 [*Hildreth et al.*, 1984]), Aira (400 km^3 [*Aramaki*, 1984]), and Taupo (155 km^3 [*Self*, 1983]). All of these volumes are likely to be underestimates (C. Wilson, personal communication, 1991). The principal difference between the eruption conditions on Venus and on Earth is the surface pressure [*Head and Wilson*, 1986]. On Venus it is 9 MPa, compared with 0.1 MPa for Earth. This difference strongly affects the expansion of the exsolved bubbles and hence the stress in the bubble walls. On Venus the stresses generated in this way are a factor of between 10^3 and 10^4 smaller than they are on Earth. Explosions produced by failure of the bubble walls are therefore less likely on Venus. This difference may explain why large domes appear to be commoner on Venus than they are on Earth. The only domes known that are of comparable size to those on Venus are within the Yellowstone caldera, whose volumes are 75-200 km^3 [*Hildreth et al.*, 1984; C. Wilson, personal communication, 1991]. Of the terrestrial volcanoes that are known to have erupted large volumes of silicic magma, all but one are above subduction zones, where hydrous minerals in the oceanic crust are being transported into the hot mantle by the subducting slabs. The water released from these slabs lowers the viscosity of silicic melts by as much as a factor of 10^8 by breaking the bonds that link the SiO_2 tetrahedra and so allows crystals of olivine, pyroxene, amphibole, and plagioclase to sink through the magma as it cools. Separation of such crystals increases the SiO_2 content of the melt. When the magmas erupt, most of the water is exsolved as bubbles and lost from the magma, whose viscosity then increases greatly. The one eruption that is not associated with an island arc is Yellowstone, where the volcanism results from a plume, and the silicic magma is generated by melting the continental crust. However, the crust involved was itself originally produced by island arcs earlier in Earth's history.

On Venus there is no evidence that domes are related to subduction or that subduction transports water into the mantle. Indeed the absence of volcanism associated with the trench systems of eastern Aphrodite strongly suggests that no such transport occurs. It is nonetheless possible that the dome magmas were originally water saturated. At present, no tectonic or volcanic processes are known to operate on Venus that could produce wet magmas, but the mechanisms involved may become clearer when the evolution of Venus is better understood.

Acknowledgments. We wish to thank J. Brodholt, J. Fink, H. Huppert, M. Stasiuk, S. Webb, and C. Wilson for their help, and the Natural Environment Research Council and the Royal Society for support. The paper was written while D. McKenzie was at Scripps Institution of Oceanography, supported by the Cecil and Ida Green Foundation and by the Scripps Institution of Oceanography. Earth Sciences Contribution 2240.

REFERENCES

Aramaki, S., Formation of the Aira Caldera, southern Kyushu, ~ 22,000 years ago, *J. Geophys. Res., 89*, 8485-8501, 1984.

Blake, S., Viscoplastic models for lava domes, in *Lava Domes and Flows, IAVCEI Proceedings in Volcanology*, vol. 2, edited by J. H. Fink, pp. 88-126, Springer-Verlag, Berlin, 1990.

Chadwick, W. W., R. J. Archuleta, and D. A. Swanson, The mechanics of ground deformation precursory to dome-building extrusions at Mount St. Helens 1981- 1982, *J. Geophys. Res., 93*, 4351-4366, 1988.

Fink, J. H. (Ed.), The emplacement of silicic domes and lava flows, *Spec. Pap. Geol. Soc. Am. , 212*, 1987.

Fink, J. H., and R. W. Griffiths, Radial spreading of viscous-gravity currents with solidifying crust, *J. Fluid Mech., 221*, 485-509, 1990.

Ford, P. G. , and G. H. Pettengill, Venus topography and kilometre-scale slopes, *J. Geophys. Res.*, this issue.

Head, J. W., and L. Wilson, Volcanic processes and landforms on Venus: Theory, predictions and observations, *J. Geophys. Res., 91*, 9407-9447, 1986.

Head, J. W., D. B. Campbell, C. Elachi, J. E. Guest, D. McKenzie , R. S. Saunders, G. G. Schaber, and G. Schubert, Venus volcanism: Initial analysis from Magellan data, *Science, 252*, 276-288, 1991.

Hildreth, W., R. L. Christiansen, and J. R. O'Niel, Catastrophic isotope modification of rhyolite magma at times of caldera subsidence, Yellowstone Plateau volcanic field, *J. Geophys. Res., 89*, 8339-8369, 1984.

Huppert, H. E., The propagation of two-dimensional and axisymmetric viscous gravity currents over a rigid horizontal surface, *J. Fluid Mech., 121*, 43-58, 1982.

Huppert, H. E., J. B. Shepard, H. Sigurdsson, and R. S. J. Sparks, On lava dome growth, with application to the 1979 lava extrusion of the Soufriere of St. Vincent, *J. Volcanol. Geotherm. Res., 14*, 199-222, 1982.

Iverson, R. M., Lava domes modelled as brittle shells that enclose pressurized magma, with application to Mount St. Helens, in The emplacement of silicic domes and lava flows, edited by J. H. Fink, *Spec. Pap. Geol. Soc. Am., 212*, 47-69, 1987.

Merrill, R. B., J. K. Robertson, and P. J. Wyllie, Melting reactions in the system $NaAlSi_3O_8$-$KAlSi_3O_8$-SiO_2-H_2O to 20 kilobars compared with results for other feldspar–quartz–H_2O and rock–H_2O systems, *J. Geol., 78*, 558-569, 1970.

Nye, J. F., The mechanics of glacier flow, *J. Glaciol., 2*, 82-93, 1952.

Pavri, B., J. W. Head, K. B. Klose, and L. Wilson, Steep-sided domes on Venus: Characteristics, geological setting, and eruption conditions from Magellan data, *J. Geophys. Res.*, this issue.

Rose, W. I., and C. A. Chesner, Dispersal of ash in the great Toba eruption, 75 ka, *Geology, 15*, 913-917, 1987.

Self, S., Large-scale phreatomagmatic silicic volcanism: a case study from New Zealand, *J. Volcanol. Geotherm. Res., 17*, 433-469, 1983.

Surkov, Yu. A., V. L. Barsukov, L. P. Moskalyeva, V. P. Kharyukova, and A. L. Kermurdzhian, New data on the composition, structure, and properties of Venus rock obtained by Venera 13 and Venera 14, *Proc. Lunar Planet. Sci. Conf. 14th*, Part 2, *J. Geophys. Res., 89*, suppl., B393-B402, 1984.

Webb, S. L., and D. B. Dingwell, Non-Newtonian rheology of igneous melts at high stresses and strain rates: Experimental results for rhyolite, andesite, basalt, and nephelinite, *J. Geophys. Res., 95*, 15,695-15,701, 1990.

P. G. Ford, F. Liu, and G. H. Pettengill, Center for Space Research, Room 37- 641, Massachussetts Institute of Technology, Cambridge, MA 02139.

D. M^{c}Kenzie, Bullard Laboratories, Madingley Road, Cambridge CB3 OEZ, England.

(Received September 30, 1991;
revised June 11, 1992;
accepted June 11, 1992.)